REFORMED NATURAL GAS, ACID MATRIX FUEL CELL BATTERIES

D. Y. C. Ng and D. K. Fleming

Institute of Gas Technology
3424 South State Street
Chicago, Illinois 60616

INTRODUCTION

This paper is a condensed report on the first 4 years of the low-temperature acid electrolyte fuel cell program sponsored at the Institute of Gas Technology by a group of gas utilities. The purpose of the program is to develop an economical, air-breathing fuel cell powered by natural gas.

Because methane is relatively unreactive electrochemically, this program emphasized steam reforming of the natural gas to a hydrogen-rich fuel for the cell. The fuel cell was adapted from the hydrogen-oxygen cell to make it operate on dilute (and poisoning) reformed natural gas and air. Acid electrolyte was required because it is compatible with the carbon dioxide that is present in the fuel.

The program was subdivided into three related technical categories:

1. Conditioning of the natural gas fuel
2. Electrode catalyst reduction and life evaluation
3. Fuel cell stack design and engineering

These technical areas are discussed below, along with another major point – overall fuel cell cost.

HYDROGEN GENERATOR DEVELOPMENT

A novel three-stage process was developed for conversion of low-pressure natural gas into a hydrogen-rich fuel suitable for use in acid fuel cells. The process was translated into efficient, integrated, prototype hydrogen generators which produced a fuel containing less than 20 ppm of carbon monoxide. The process and equipment has been described in detail in earlier papers.[5, 6]

Development of the hydrogen generator has been temporarily suspended. Using better anode catalysts, other investigators have successfully operated acid fuel cells with feeds containing as much as 10% carbon monoxide at 300°F with little poisoning effect.[2] However, the hydrogen generation process will probably still be desirable for the operation of fuel cells at the more moderate temperatures that minimize corrosion and with electrodes that have a lower platinum content.

ELECTRODE EVALUATION

The primary goal of the program was the development of economical fuel cells operating on reformed natural gas and air. The noble metal content of the electrode was the primary cost in the acid fuel cell at the beginning of the program. Figure 1 presents the reduction of the noble metal content during the 4 years. At the start of the program, available electrodes contained 80 mg Pt/sq cm – a catalyst utilization of 250 troy oz/kw at obtainable power levels on hydrogen and oxygen.

At the end of 1966, utilization had improved to less than 1 troy oz/kw while operating on reformed natural gas and air.

American Cyanamid Company's introduction of thin-screen electrodes at this meeting in 1963[3] and its recent work on lower loading electrodes are apparent in Figure 1. The intermediate performance improvements reflect better test cell design, improved operating conditions, and higher power densities.

These electrodes have been long-lived. Figure 2 shows the lifetime of one of our first immobilized phosphoric acid, capillary matrix cells operating at 90°C. The performance of this cell was relatively constant if matrix deterioration is discounted. Both electrodes in this test were American Cyanamid Type AA-1 containing 9 mg Pt/sq cm and operating at a 40 ma/sq cm current density.

Table 1 lists the lifetimes and performances of representative small-cell tests. Reduced anode loadings do not cause appreciable power loss with 20-ppm carbon monoxide in the dilute fuel, but the tolerance to higher carbon monoxide dosages is not yet known. The reduced catalyst content at the cathode, however, does cause a noticeable power reduction.

Some of the tests listed in Table 1 were short-term (3 months or less) because the electrodes could not be recovered after dismantling the cell. Some of the low-loading electrodes do not separate readily from deteriorated matrices.

Moisture management and matrix degradation were the two major problems with the small-cell tests. The most common mode of failure for these small tests was electrolyte leaching caused by insufficient moisture removal. With a good cell design and temperature control, the moisture balance is more easily maintained.

The glass-fiber matrix is slowly attacked by phosphoric acid, changing to a gel and losing its wet strength. The effect of replacing a deteriorated matrix is evident in Figure 2. Several other matrix materials have been tested without significant success. We see no clear solution to the matrix problem at the present time.

BATTERY ENGINEERING

The third phase of the low-temperature fuel cell program was the engineering and operation of multicell battery stacks. This section of the program involved the study of heat and moisture management, proper distribution of dilute fuel and oxidant, and other problems of battery operation. Studies with dual ion-exchange membrane batteries were presented earlier.[4] These efforts were abandoned in favor of immobilized electrolyte, capillary matrix batteries, which appear to hold greater promise for ultimate cost reduction. However, the heat and moisture balances are more critical with the matrix battery because of the reduced electrolyte inventory.

Figure 1 includes a line for the catalyst reduction achieved with battery operation. Because all stacks operated since 1964 contained American Cyanamid Type AA-1 electrodes (18 mg Pt/sq cm total), the improved catalyst utilization reflects improvements in power density only. The power densities obtained were 48 w/sq ft with the membrane batteries, 73.2 w/sq ft with 0.25-sq-ft matrix batteries, and 82.5 w/sq ft with larger matrix batteries. The electrode cost of the batteries lags behind that of the test cells by approximately 1 to 1-1/2 years because of electrode availability and the need for preliminary evaluation. The battery electrode costs will probably be similar to those of the present small-cell electrode costs when the low-noble-metal-content electrodes are operated in multicell stacks.

Table 1. REPRESENTATIVE SMALL-CELL (4 sq in.) TESTS

Noble Metal Content, ma/sq cm		Max. Power Density on RNG/Air, mw/sq cm	Noble Metal Utilization at Max. Power, troy oz/kw	Operating Conditions (RNG/O_2)				Comments
Anode	Cathode			Current Density, ma/sq cm	Potential, mv	Lifetime, days	Matrix Changes	
9	9	68	8.5	40	680	600†	2	Older cell design
9	9	75	7.7	100	720	135†	2	Improved cell gas distribution and IR
9	2.5	58	6.4	40	720	239†	1	Older cell design
9	1	50	6.4	40	700	32†	1	High air polarization
1	9	72	4.5	40	700	55	0	Anode not recoverable
0.5	9	70	4.4	40	720	58	0	Anode not recoverable
0.25	2.5	64	1.4	40	700	78	0	Very stable
0.25	1	(50)	0.8					Estimated from above tests

†Determined from other tests with these electrodes.
Test continuing on January 1, 1967.

The basic matrix fuel cell unit is similar in all of the sizes tested in this program. Figure 3 shows an exploded view of the cell design. The electrolyte is absorbed in Whatman GF-82 glass-fiber paper that is 25 mils thick. The edges of this glass-fiber matrix are impregnated with Kel-F to minimize electrolyte leakage through the exposed edges of the cell. The fuel compartment is enclosed by an ethylene-propylene-terpolymer gasket and has interfaces at the anode, which is adjacent to the matrix, and at the bipolar plate, which it shares with the next cell. Fuel flows into the cell from manifold ports in the top edge and over the face of the cell. Spent fuel is exhausted through a single outlet at the bottom. The cathode compartment is similar.

Matrix cells of this construction are stacked into a battery. The bipolar plate acts as a gas separator and an electrical connector between the adjacent cells. The resulting battery is electrically connected in series. The overall size of a 0.25-sq-ft cell is 5.5 x 9.6 x 0.100 in. with a 4.7 x 7.7 in. active area. The larger cell size is 12 x 13 x 0.100 in. with a 9.5-in.-square active area. Based on the maximum power obtained from the larger cells, exclusive of end plates and fittings, the unit weight of the stack is about 15 lb/kw and the unit volume is about 0.18 cu ft/kw. At design power levels of 55 w/sq ft, the specific weight and volume increase to 22 lb/kw and 0.26 cu ft/kw. Figure 4 is a photograph of the components of a single cell.

The heat and moisture balances within the cell were studied by computer analysis. Partial differential equations modeling the heat and mass flows were solved by the finite difference technique. For the geometry and operating conditions used, the calculations indicated that the gas flow required to remove the heat generated in the cell was an order of magnitude greater than that required to remove the product water. Therefore, the excess heat must be removed by a separate mechanism.

Ethylene glycol circulating through the hollow end plates of five-cell modules cools the stack, as illustrated schematically in Figure 5. At 100 amp/sq ft current density, the temperature variation from the center cell to the end cell of a module is 45°F. Based on published correlations for heat transfer in a fuel cell battery,[1] the effective thermal conductivity in the direction of current flow is only about 0.11 Btu/hr-ft-°F for this geometry. The tortuous path for heat removal probably causes the low conductivity. Each cell in the module operates at the acid concentration which is in equilibrium, at the individual cell temperature, with the gas flows.

Cell modules are connected electrically in series to produce the desired output. Figure 6 illustrates a three-module 500-watt battery which was successfully operated near the end of the reporting period. The output of this battery was 7.6 volts at 70 amp of gross current.

A typical polarization curve for a five-cell module is shown in Figure 7. The stack voltage at 100 amp/sq ft current density was 3.3 volts or 0.66 volt per cell. The maximum power output of this stack was 243 watts at 90 amp (144 amp/sq ft). At 70-amp current, the maximum cell-to-cell deviation was 2.5%, although the deviation was greater at higher current densities. Maldistribution was evident at these conditions, as indicated by the nonlinearity of Figure 7.

The flow distribution across the face of the cell was checked by assemblying a dummy cell without electrodes. The matrix was soaked with lead acetate, the desired flow rate was established, and a small quantity of hydrogen sulfide was injected into the inlet line. The hydrogen sulfide reacts with the lead acetate until the hydrogen sulfide is consumed, leaving a dark pattern which indicates the flow regime over the face of the cell.

Gas distribution can also be determined by fuel utilization efficiency curves such as those shown in Figure 8. In this graph, the flow rate is expressed in multiples of the stoichiometric fuel requirements. Figure 8 indicates that fuel utilizations greater

than 50% may be expected from this cell design at higher current densities without excessive penalty. However, the design should be improved to displace the knee of these utilization curves closer to the stoichiometric fuel requirements.

FUEL CELL COSTS

The basic raw material costs of fuel cell batteries and test cells operated in this program are tabulated below as a function of date.

Table 2. BASIC MATERIAL COSTS OF IGT LOW-TEMPERATURE FUEL CELLS AND BATTERIES

Component	Jan. 1963[a]	March 1964[b]	April 1965[c]	March 1966[d]	Dec. 1966[e]
	$/kw				
Precious Metal (catalyst)	23,000	2,800	1,520	775	80
Electrode Screen	23,000	141	79	40	57
Bipolar Plates	1,140	230	128	65	93
Membranes	385	360	220	--	--
Gaskets, etc.	53	50	28	10	14

[a]Original IEM battery, 18.7 w/sq ft with 72 g/sq ft electrodes on Pt gauze.

[b]Improved IEM battery, 20 w/sq ft with American Cyanamid AA-1 electrodes.

[c]13-cell, 0.25-sq-ft IEM battery with American Cyanamid AA-1 electrodes at 35.5 w/sq ft.

[d]5-cell, 0.25-sq-ft matrix battery with American Cyanamid AA-1 electrodes at 72 w/sq ft.

[e]4-sq-in. matrix cell using an American Cyanamid BA-1/4 anode and BA-2C cathode at 50 w/sq ft(estimated).

Table 2 lists basic material costs only and does not include the value added by manufacture. The reduction in catalyst cost, in line with Figure 1, has been significant. At the present state of development, the value of the other metallic components of this cell is greater than that of the catalyst. If these subsidiary costs can be reduced, the fuel cell should soon become an economic reality.

The fuel cell catalyst costs do not require further reduction. The range of $100/kw is probably less than required for an economic fuel cell because the platinum catalyst is not destroyed in the cell operation. Since the catalyst values may be recovered for a nominal charge (similar to current practice with petroleum refinery catalysts), the platinum is essentially nondepreciable. In addition, the platinum is a highly fluid asset and may be used as collateral for low-interest bonds. Under gas industry economics, the annual costs for this catalyst should be about 7%. Figure 9 presents the annual charge, including platinum recovery, for several electrode combinations. The assumption has been made that the peak power density currently obtainable with these platinum loadings will be the future design basis.

Figure 9 illustrates that the true annual cost of the catalyst is low and that higher catalyst loadings may be possible, depending on the overall economics of the system.

ACKNOWLEDGMENTS

The authors wish to thank Southern California Gas Company, Southern Counties Gas Company, and Consolidated Natural Gas Service Company, Inc., sponsors of this investigation, for permission to publish these results.

LITERATURE CITED

1. Gidaspow, D., Baker, B. S., Jee, B. C. and Oliva, F., "Heat Transfer in a Fuel Cell Battery – Maximum Battery Temperatures." Paper No. C-213 presented at the 17th Meeting of the International Committee of Electrochemical Thermodynamics and Kinetics, CITCE, Tokyo, September 5-13, 1966.

2. Haldeman, R. G., "Electrode-Matrix Materials." Paper presented at the 21st Annual Power Sources Conference, Atlantic City, N.J., May 16-18, 1967.

3. Haldeman, R. G., Colman, W. P., Langer, S. H. and Barber, W. A., "Thin Fuel Cell Electrodes," in Young, G. J. and Linden, H. R., Eds., Fuel Cell Systems, Advances in Chemistry Series No. 47, 106-15. Washington, D. C.: American Chemical Society, 1965.

4. Leitz, F. B., Glass, W. and Fleming, D. K., "Performance of a Reformed Natural Gas-Acid Fuel Cell System. Part II – Fuel Cell Battery," in Baker, B. S., Ed., Hydrocarbon Fuel Cell Technology, 37-50. New York: Academic Press, 1965.

5. Meek, J. and Baker, B. S., "Hydrogen From Natural Gas for Fuel Cells," in Young, G. J. and Linden, H. R., Eds., Fuel Cell Systems, Advances in Chemistry Series No. 47, 221-31. Washington, D. C.: American Chemical Society, 1965.

6. Meek, J., Baker, B. S. and Allen, A. C., "Performance of a Reformed Natural Gas-Acid Fuel Cell System. Part I – Hydrogen Generator Design," in Baker, B. S., Ed., Hydrocarbon Fuel Cell Technology, 25-35. New York: Academic Press, 1965.

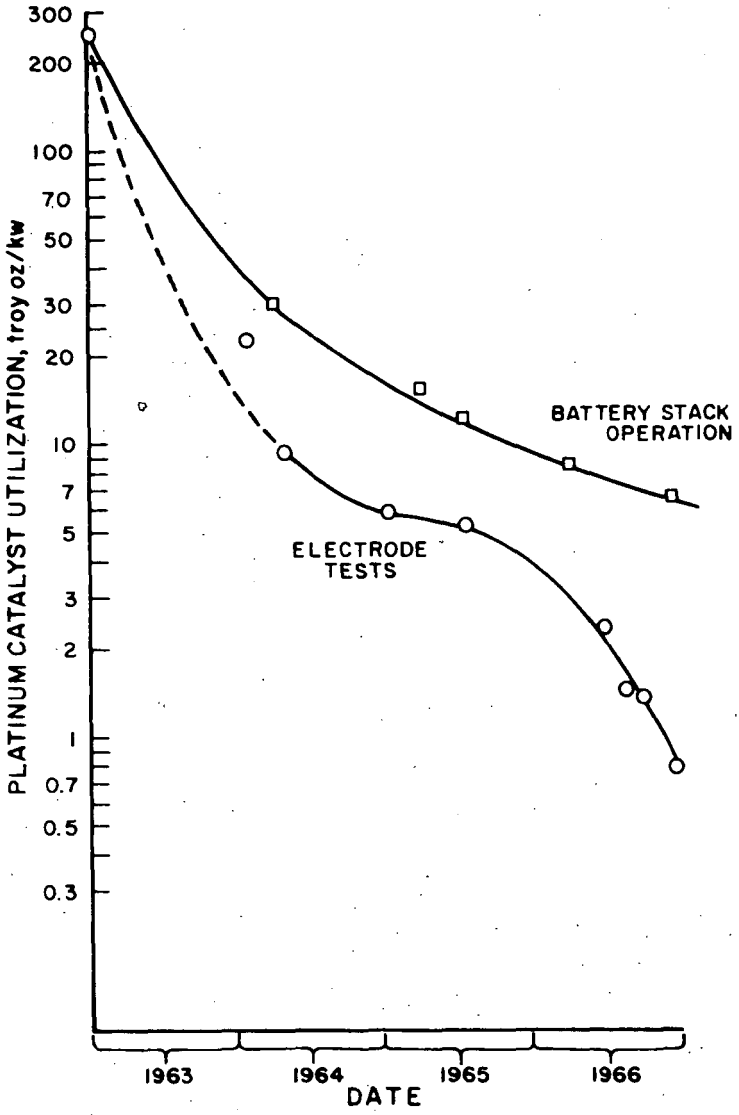

Figure 1. IMPROVEMENT IN CATALYST UTILIZATION

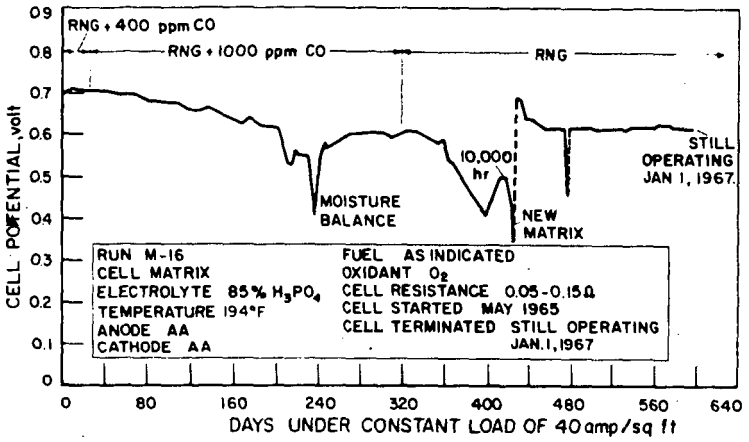

Figure 2. LIFETIME PERFORMANCE OF TEST CELL M-16 (AA-1 Electrodes, Low Current Density)

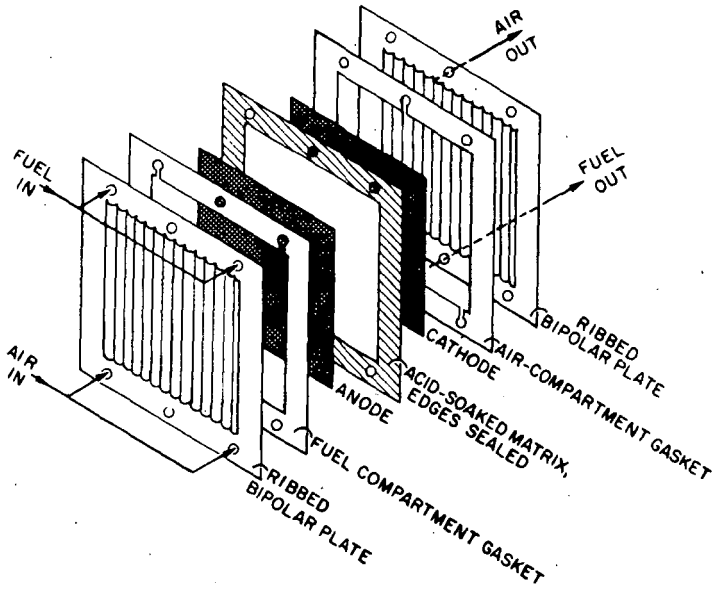

Figure 3. EXPLODED VIEW OF A SINGLE CELL

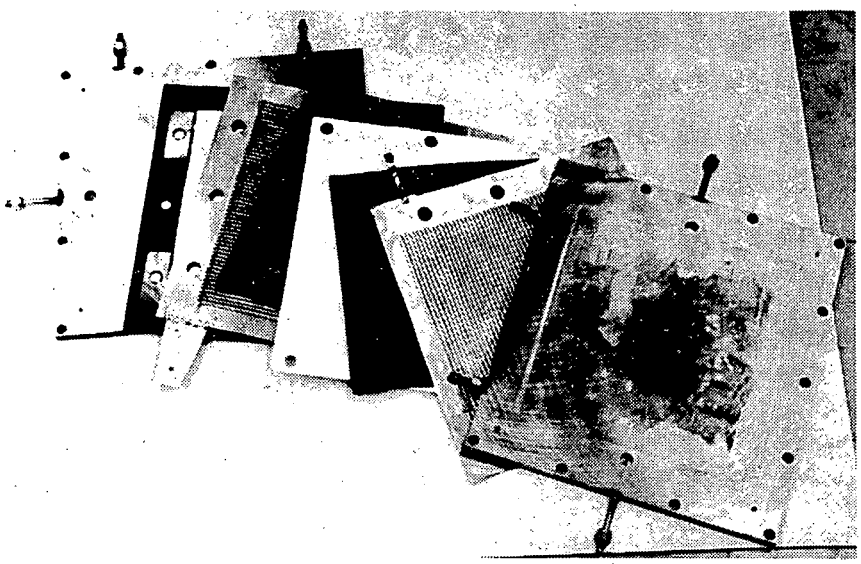

Figure 4. VIEW OF 0.63-sq-ft CELL COMPONENTS

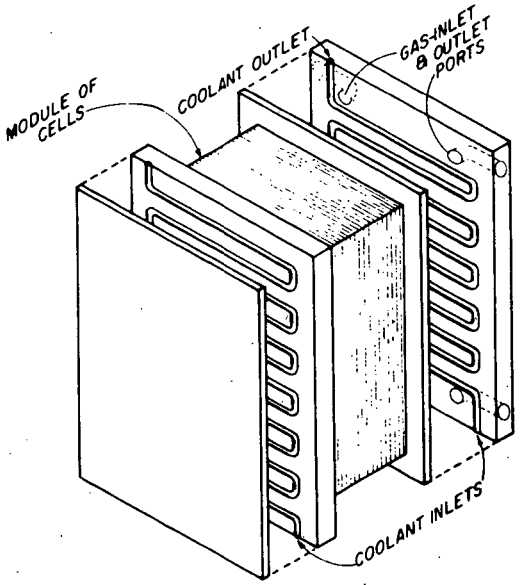

Figure 5. SCHEMATIC REPRESENTATION OF MODULAR CELL COOLING

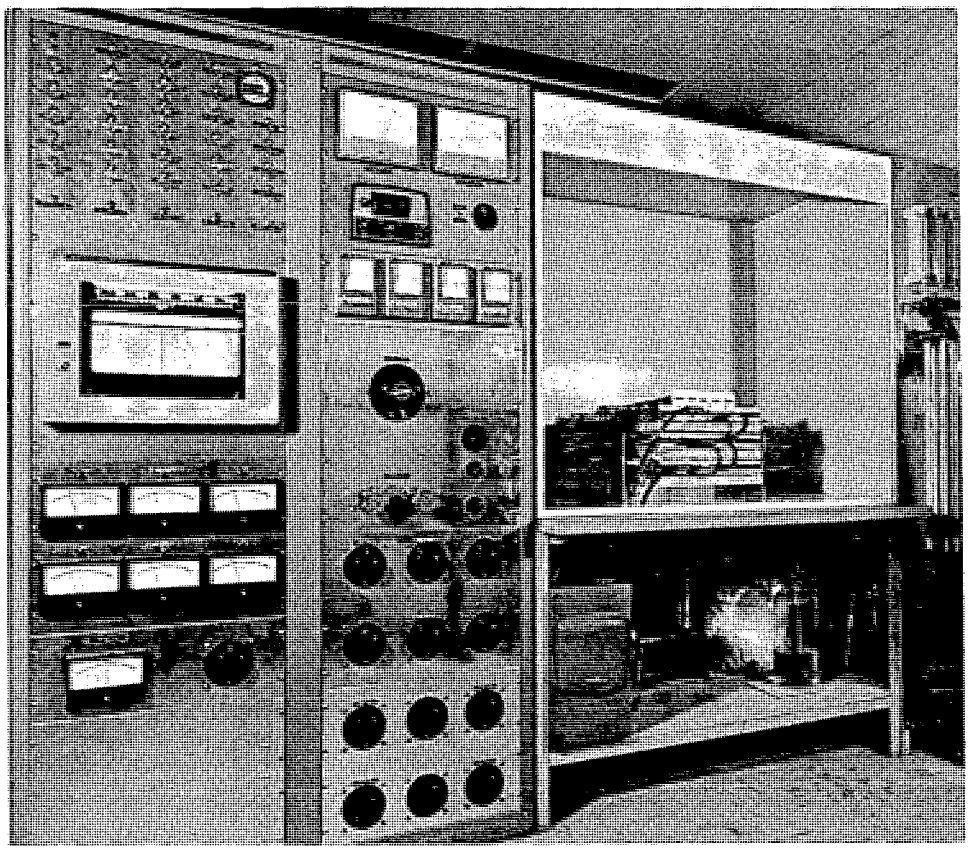

Figure 6. TEST STATION WITH 500-WATT MATRIX FUEL CELL BATTERY

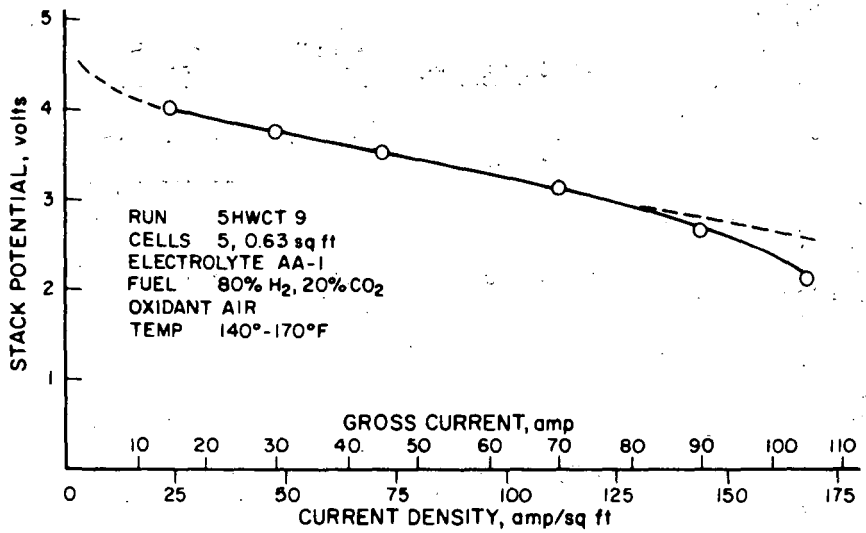

Figure 7. POLARIZATION CURVE FOR LARGE-CELL STACK

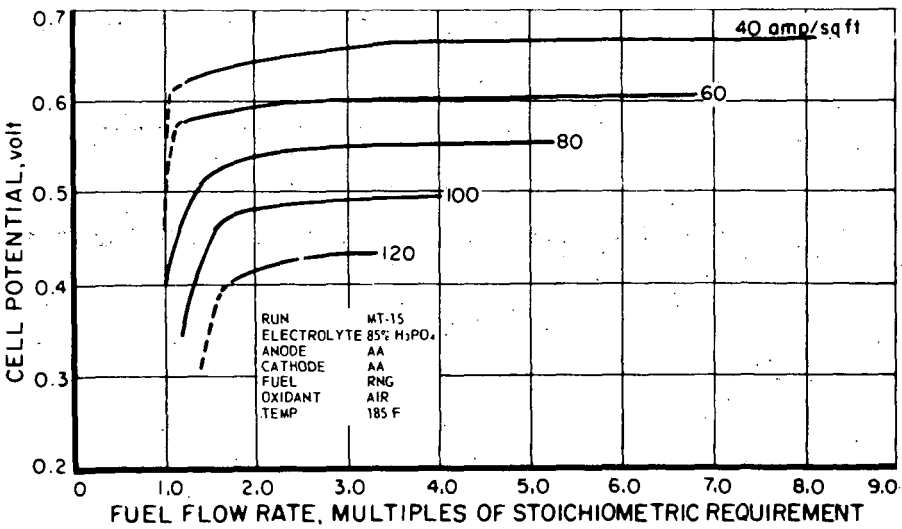

Figure 8. FUEL UTILIZATION

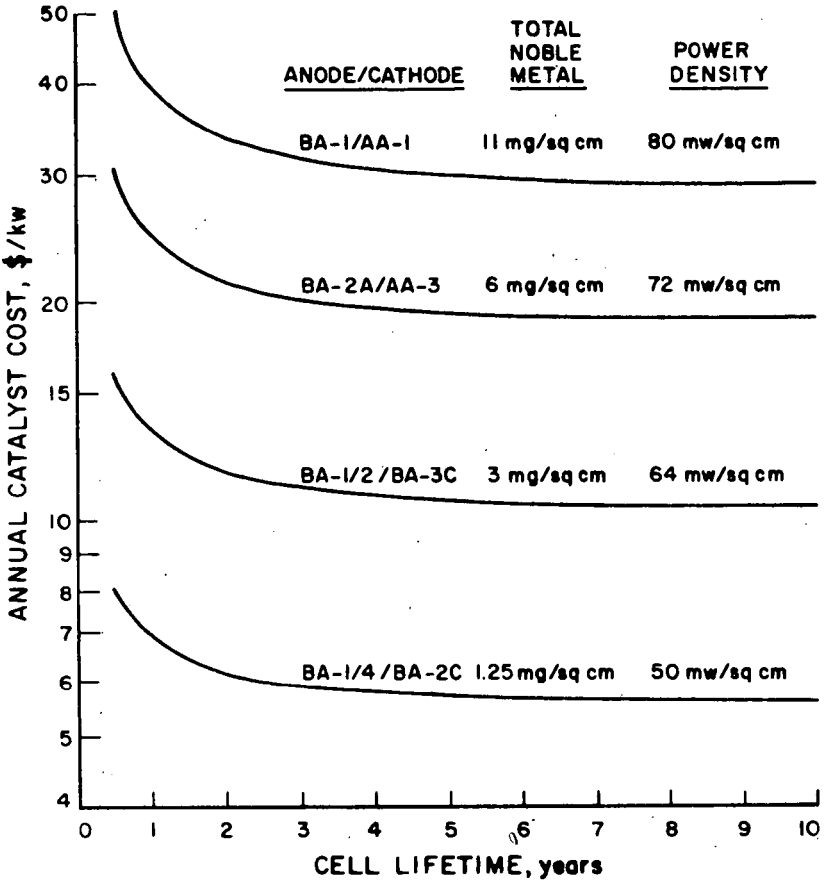

Figure 9. ANNUAL CATALYST COST FOR ELECTRODE CONDITIONS:
Platinum at $90/troy oz
Rhodium at $180/troy oz
Capital at 7%
Noble-Metal Recovery at $1/troy oz